

Annihilating Dark Matter Search with 12 Years of Fermi LAT Data in Nearby Galaxy Clusters

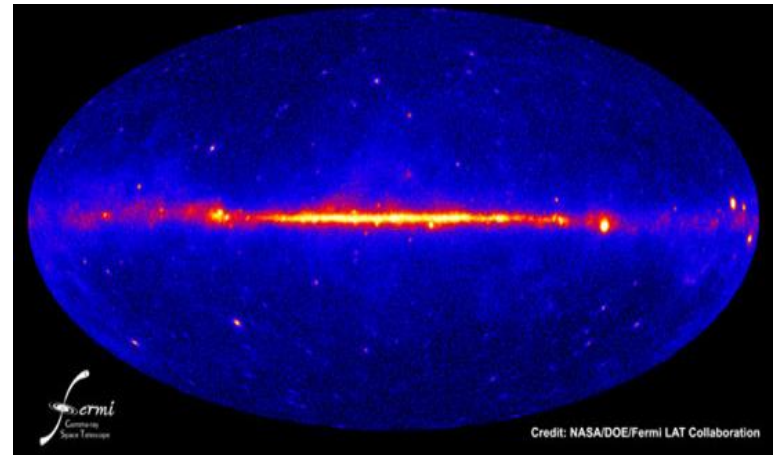
Charles Thorpe-Morgan, Denys Malyshev, Christoph-Alexander Stegen, Andrea Santangelo, Josef Jochum

IDM, 21.07.2022



Structure:

- Background
 - Dark matter signals
 - Dark matter profiles
 - Targets for indirect DM search
- Method
 - Target selection
 - Dark matter model
 - Likelihood fitting
- Results
 - Limits from clusters

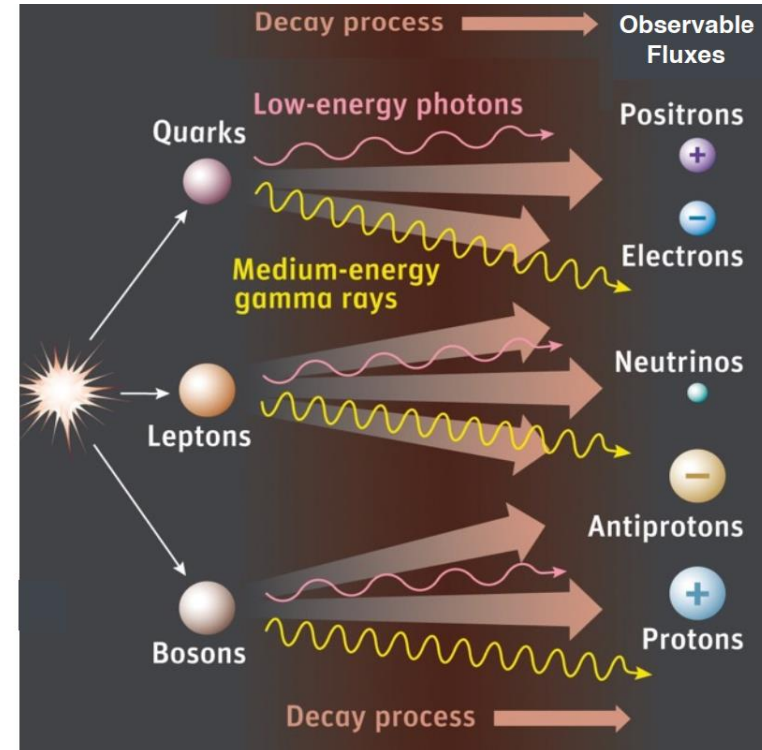




Dark Matter Signals (Indirect Detection)

- Detecting Standard Model particles formed from decay/annihilation of DM
- Photons provide directionality and energy information
- Additional photons from secondary interactions of SM particles (Inverse Compton, Bremsstrahlung etc.)
- Photons form a detectable excess following the morphology of DM

DM annihilation/decay



Source: NASA website

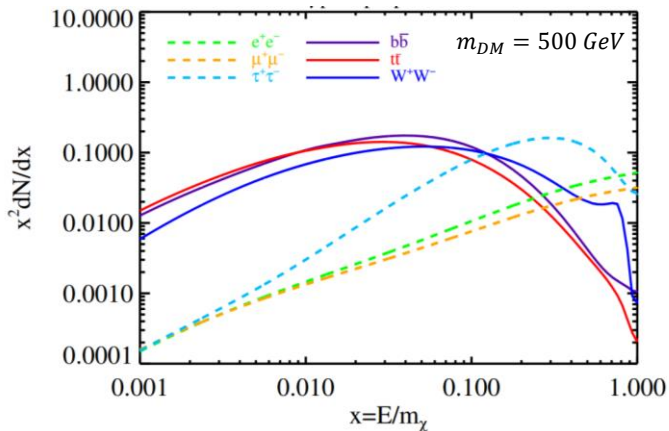


Expected “Flux” of Dark Matter Signals (Annihilation)

$$\frac{d\phi(\Delta\Omega, E)}{dE} = \underbrace{\frac{1}{4\pi} \frac{\langle \sigma v \rangle}{2m^2} \sum B_{ri} \frac{dN_i(E)}{dE}}_{\text{Particle Physics Term}} \times \underbrace{\int_{\Delta\Omega} \int_{l.o.s} \rho^2 dl d\Omega}_{\text{Astrophysical Term}}$$

Particle Physics Term

- Purely dependent on the nature of DM
- Differential term represents the spectral energy distribution
- Energy spectra of γ -rays from products



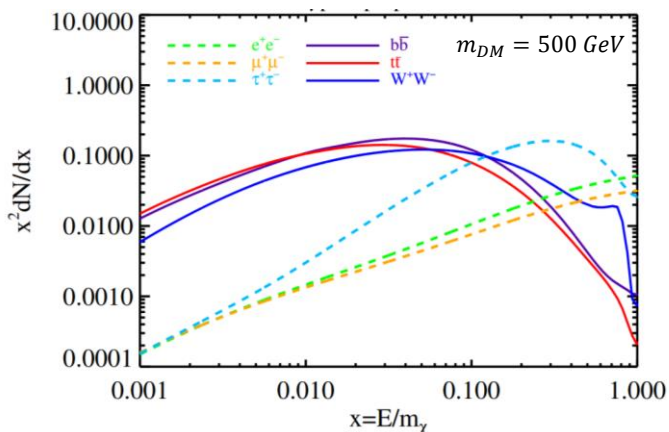


Expected “Flux” of Dark Matter Signals (Annihilation)

$$\frac{d\phi(\Delta\Omega, E)}{dE} = \underbrace{\frac{1}{4\pi} \frac{\langle \sigma v \rangle}{2m^2} \sum B_{ri} \frac{dN_i(E)}{dE}}_{\text{Particle Physics Term}} \times \underbrace{\int_{\Delta\Omega} \int_{l.o.s} \rho^2 dl d\Omega}_{\text{J-factor}}$$

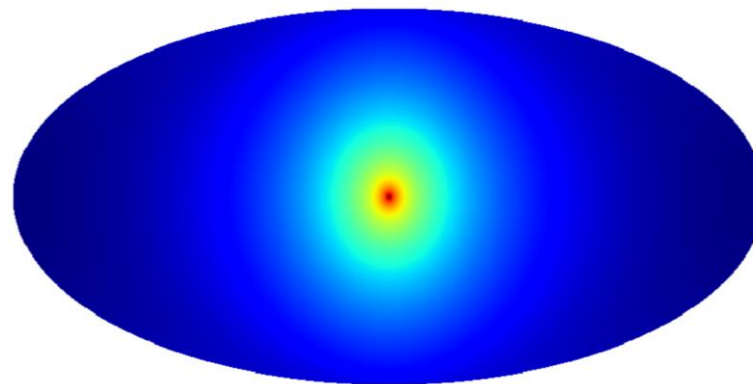
Particle Physics Term

- Purely dependent on the nature of DM
- Differential term represents the spectral energy distribution
- Energy spectra of γ -rays from products



J-factor

- Purely astrophysics contributions
- l.o.s integral of DM column density
- Defined by the morphology of DM



Source: Charles, E., 2017, A Review of Indirect Dark Matter Searches



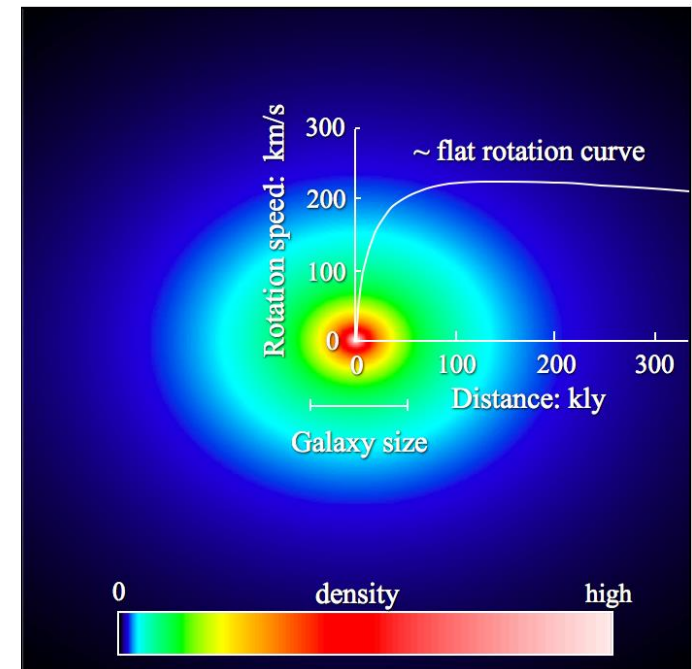
Dark Matter Profiles

- Flux heavily dependent on density profile (square dependence)
- Generalised Navarro-Frenk-White
 - Based on standard NFW
 - Profile tailored to object from observations
 - Parameters reported in literature

$$\rho(r) = \frac{2^{\frac{\beta-\gamma}{\alpha}} \rho_s}{\left(\frac{r}{r_s}\right)^\gamma \left(1 + \left(\frac{r}{r_s}\right)^\alpha\right)^{(\beta-\gamma)/\alpha}}$$

with $\alpha = 1$; $\beta = 3$; $\gamma = 1$

- Sub-halos
 - Observed in simulations of DM formation
 - small areas of high DM concentration
 - alter the DM profile of astrophysical objects leading to a greater signal at larger radii





Dark Matter Profiles

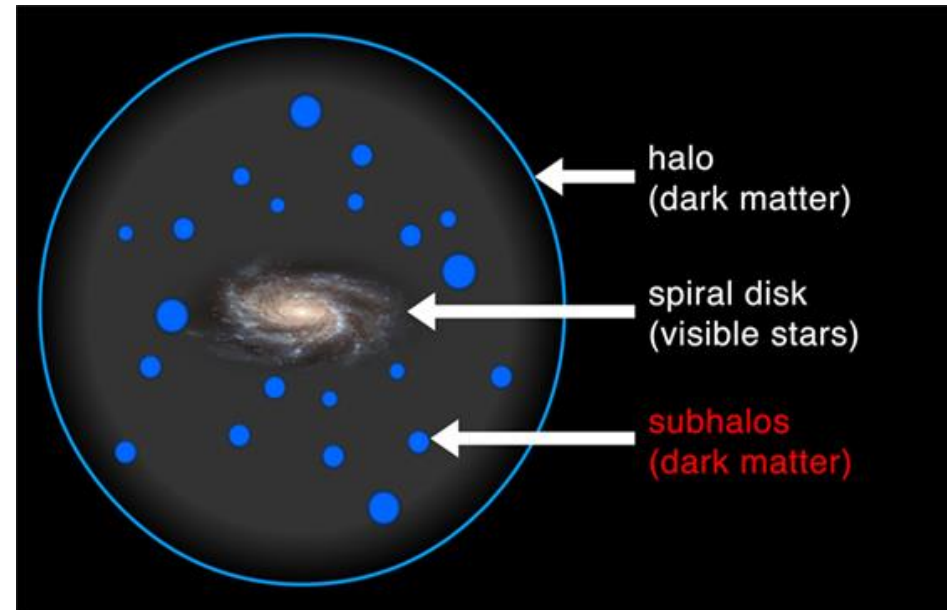
- Flux heavily dependent on density profile (square dependence)
- Generalised Navarro-Frenk-White (Zhao)
 - Based on standard NFW
 - Profile tailored to object from observations
 - Parameters reported in literature

$$\rho(r) = \frac{2^{\frac{\beta-\gamma}{\alpha}} \rho_s}{\left(\frac{r}{r_s}\right)^\gamma \left(1 + \left(\frac{r}{r_s}\right)^\alpha\right)^{(\beta-\gamma)/\alpha}}$$

with $\alpha = 1$; $\beta = 3$; $\gamma = 1$

Sub-halos

- Observed in simulations of DM formation
- small areas of high DM concentration
- alter the DM profile of astrophysical objects leading to a greater signal at larger radii

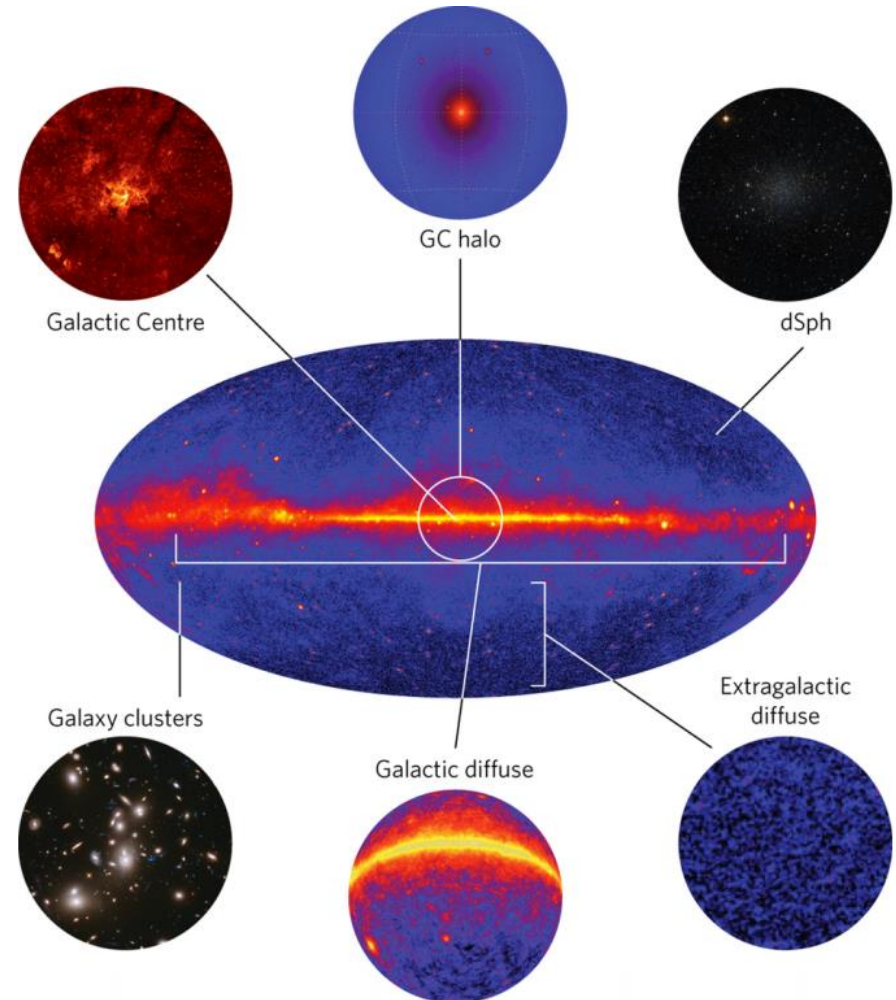




Indirect Search Targets

- Maximise J-factor
 - Must select targets that maximise ρ and angular size
 - Compromise between J-factor and foreground signal

- Observing multiple targets is essential for confirmation of the nature of a signal



Source: Charles, E., 2017, *A Review of Indirect Dark Matter Searches*



Method



Literature review and target selection

- Galaxy clusters
 - Largest Virialised objects in the universe therefore very large DM content
 - Competitive limits can be derived for those closest

- Selected 5 galaxy clusters
 - Selected only the nearest clusters ($z \leq 0.02$)
 - High galactic latitudes ($b \geq 10^\circ$)

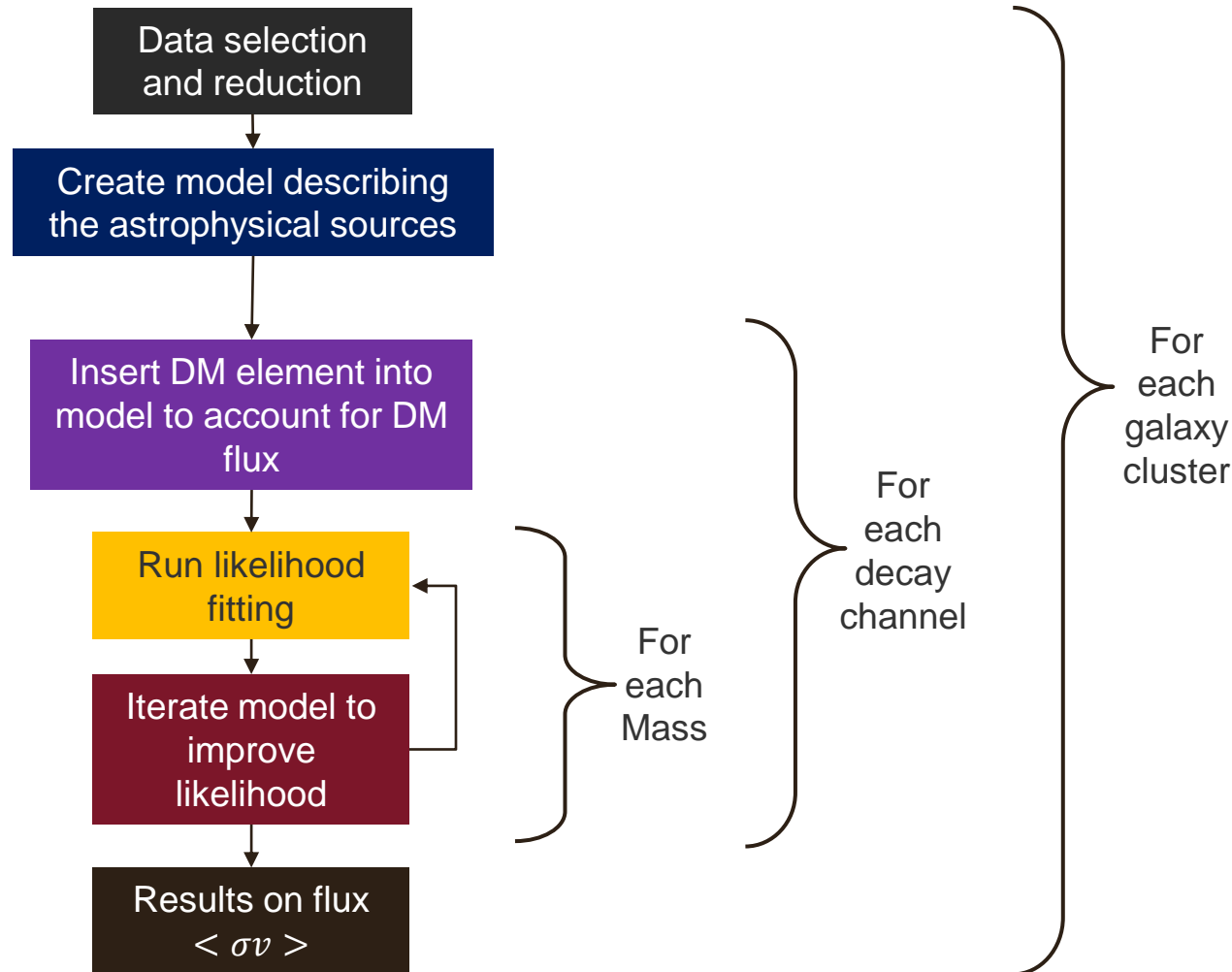
- 12 years of Fermi – LAT data
 - Limits improve as $\sim \sqrt{time}$
 - Utilised Pass 8
 - Fermi – LAT IRFS
 - Improved non-photon background rejection
 - $3^\circ \times 3^\circ$ region of Gamma-ray sky around each cluster

Cluster	R.A	Dec.	z	M_{200} [$10^{14} M_\odot$]	r_{200} Mpc
Centaurus	192.199	-41.308	0.0114	5.3	1.67
Coma	194.953	27.981	0.0231	12.9	2.24
Fornax	54.616	-35.448	0.0046	2.4	1.28
Perseus	49.947	41.513	0.0179	8.6	1.95
Virgo	187.697	12.337	0.0036	$4.2^{(a)}$	$1.08^{(b)}$

The details of clusters analysed in the Fermi-LAT likelihood analysis. (Masses and radii taken from the HIFLUGS x-ray catalogue)

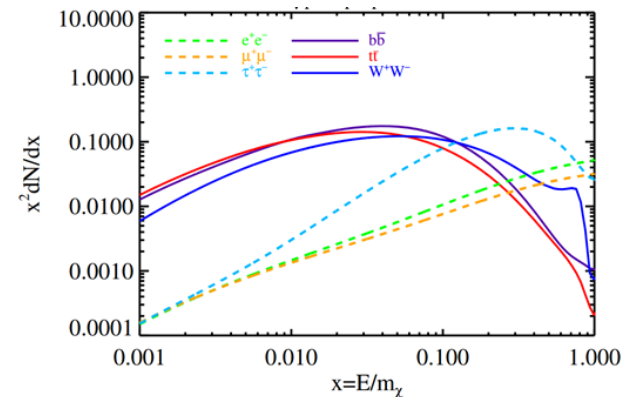
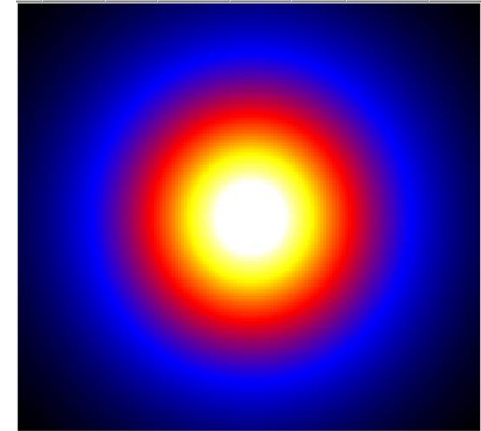


Method Overview



Dark Matter Model

- To derive limits on $\langle \sigma v \rangle$ simulated a DM flux element in the mode following the expected morphology of DM
- Simulated WIMP DM signal morphology by creating a Zhao profile for each cluster
 - Utilised multiple profiles from literature for each cluster
 - Derived from X-ray kinematics and weak lensing
 - Simulated sub-halos with the CLUMPY v.3 code
 - (Charbonnier et al.2012; Bonnavard et al. 2016; Hütten et al. 2019)
- Particle physics element
 - Mass was held constant and varied in different runs
 - $\langle \sigma v \rangle$ free parameter
 - Differential spectra from tabulated results Jeltema et al 2008
 - Channels: bb , W^+W^- , $\gamma\gamma$
 - High expected branching ratios for WIMP DM



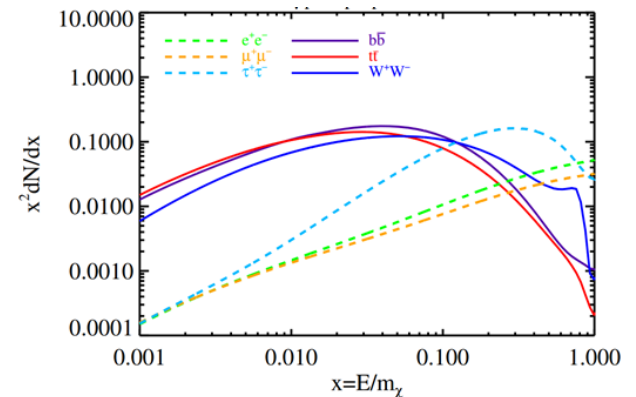
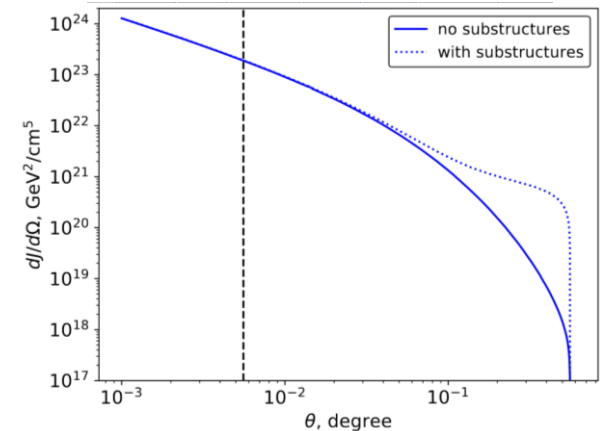


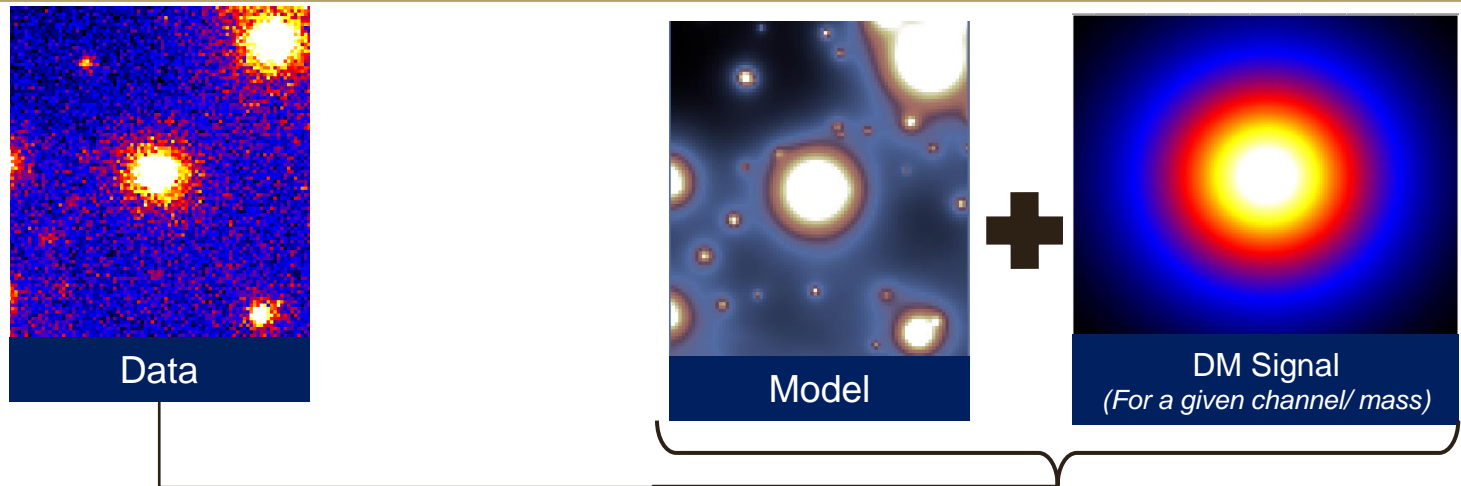
Cluster	l [deg]	b [deg]	z	r_s [kpc]	ρ_s [$10^5 M_\odot/\text{kpc}^3$]	Covariance ($\log_{10} r_s, \log_{10} \rho_s$)	Reference
Centaurus	302.398	21.561	0.0114	470	2.13	$10^{-3} \cdot \begin{pmatrix} 3.7 & -6.3 \\ -6.3 & 13.65 \end{pmatrix}$	Ettori et al. (2002)
Coma	283.807	74.437	0.0231	360	2.75	$10^{-2} \cdot \begin{pmatrix} 31.8 & -47.9 \\ -47.9 & 74.0 \end{pmatrix}$	Gavazzi et al. (2009)
Virgo	187.697	12.337	0.0036	560	0.8	$10^{-3} \cdot \begin{pmatrix} 22.5 & -39.7 \\ -39.7 & 71.4 \end{pmatrix}$	McLaughlin (1999)
Perseus	150.573	-13.262	0.0179	369	2.73	–	Simionescu et al. (2011)
Perseus	150.573	-13.262	0.0179	530	2.36	–	Ettori et al. (2002)
Fornax	236.712	-53.640	0.0046	220	1.25	–	Drinkwater et al. (2001)(DW01)
Fornax	236.712	-53.640	0.0046	98	14.5	–	Reiprich & Böhringer (2002a)(RB02)
Fornax	236.712	-53.640	0.0046	34	22.0	–	Schuberth et al. (2010)(SR10A10)

(Multiple profiles for Perseus and Fornax)

Dark Matter Model

- To derive limits on $\langle \sigma v \rangle$ simulated a DM flux element in the mode following the expected morphology of DM
- Simulated WIMP DM signal morphology by creating a Zhao profile for each cluster
 - Utilised multiple profiles from literature for each cluster
 - Derived from X-ray kinematics and weak lensing
 - Simulated sub-halos with the CLUMPY v.3 code
 - (Charbonnier et al.2012; Bonnavard et al. 2016; Hütten et al. 2019)
- Particle physics element
 - Mass was held constant and varied in different runs
 - $\langle \sigma v \rangle$ free parameter
 - Differential spectra from tabulated results Jeltema et al 2008
 - Channels: bb , W^+W^- , $\gamma\gamma$
 - High expected branching ratios for WIMP DM



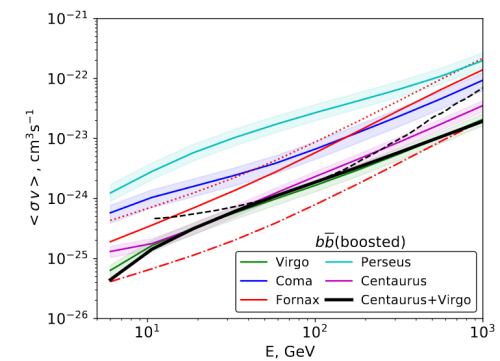
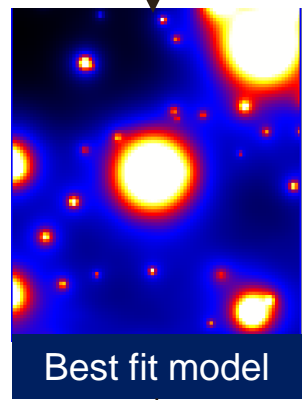


$$\mathcal{L} = e^{-N_{pred}} \prod_k \frac{m_k^{n_k}}{n_k!}$$

$e^{-N_{pred}}$ - Total counts predicted by model
 n_k - counts detected in the Kth bin
 m_k - predicted counts in the Kth bin

\mathcal{L}

(alters $\langle \sigma v \rangle$ to best match simulated DM flux in the model to the data)





Results

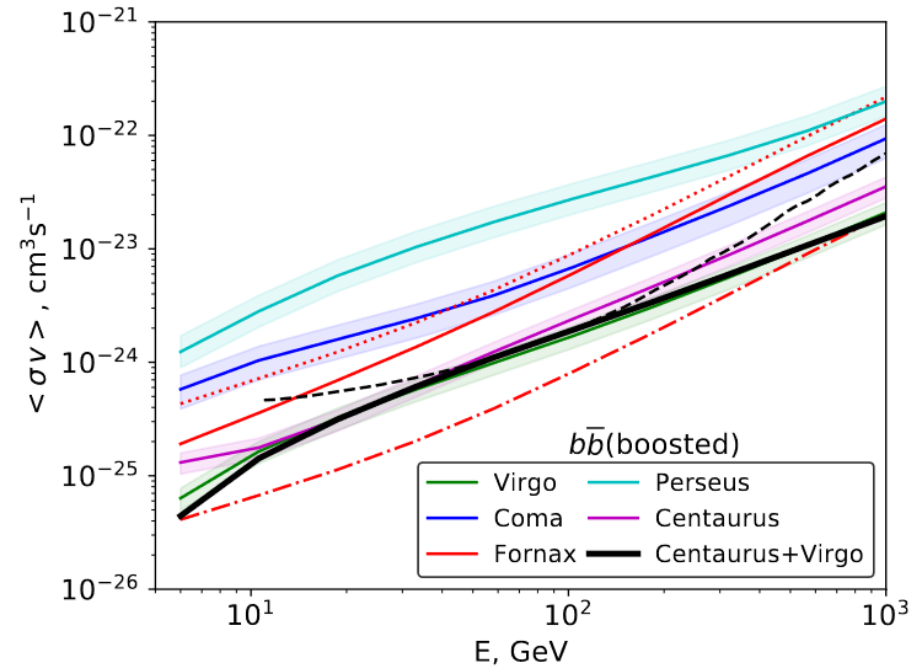
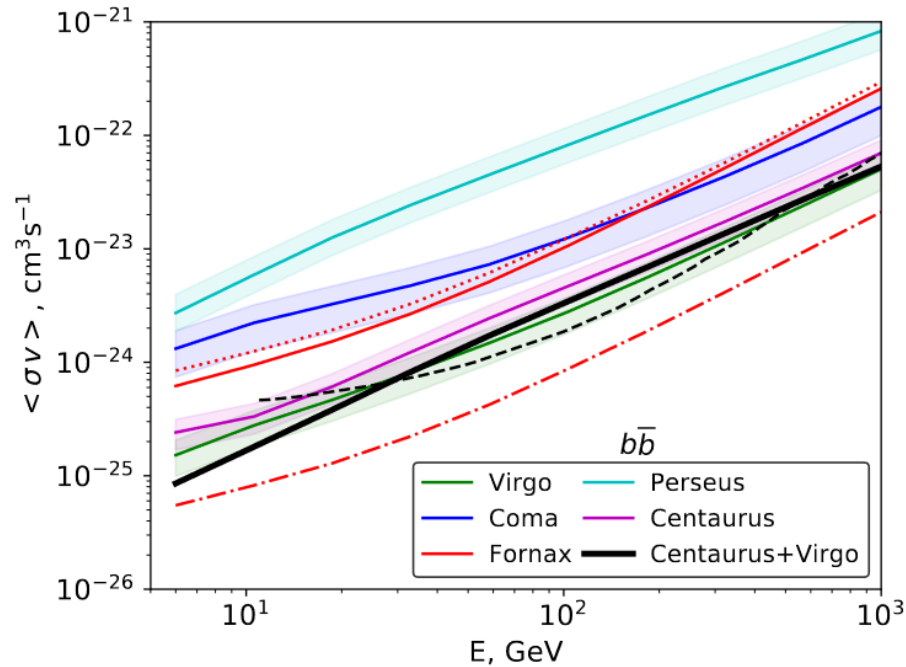
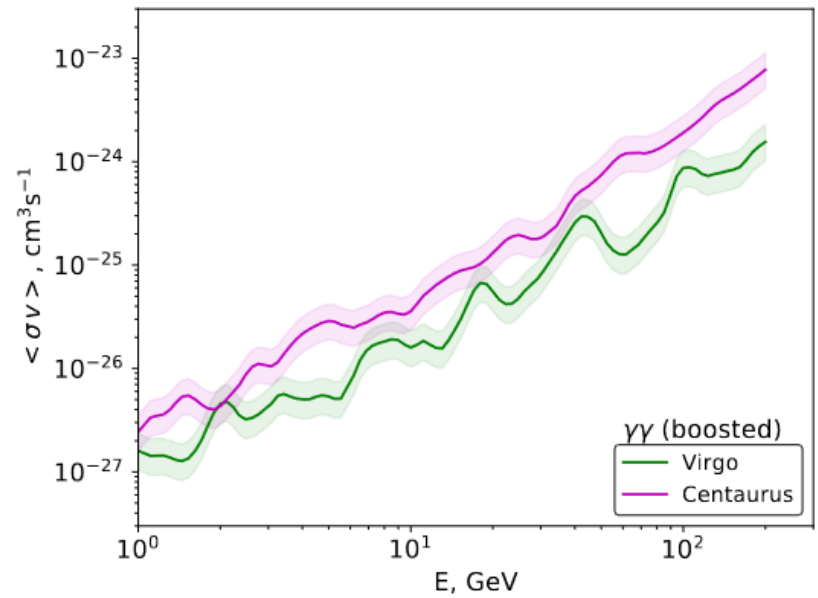
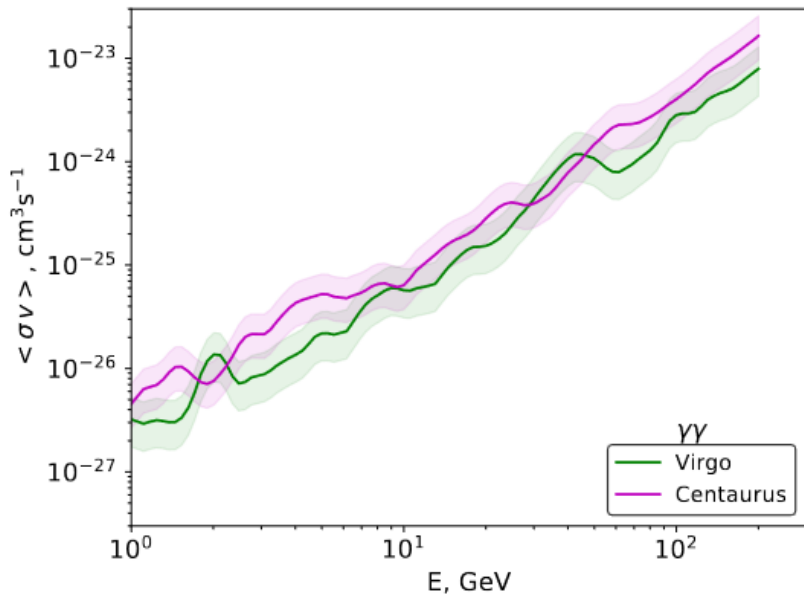
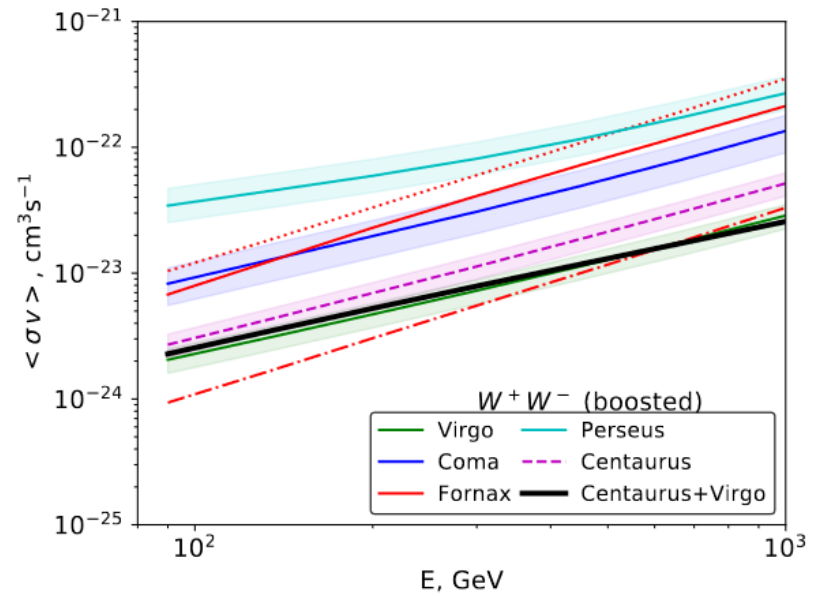
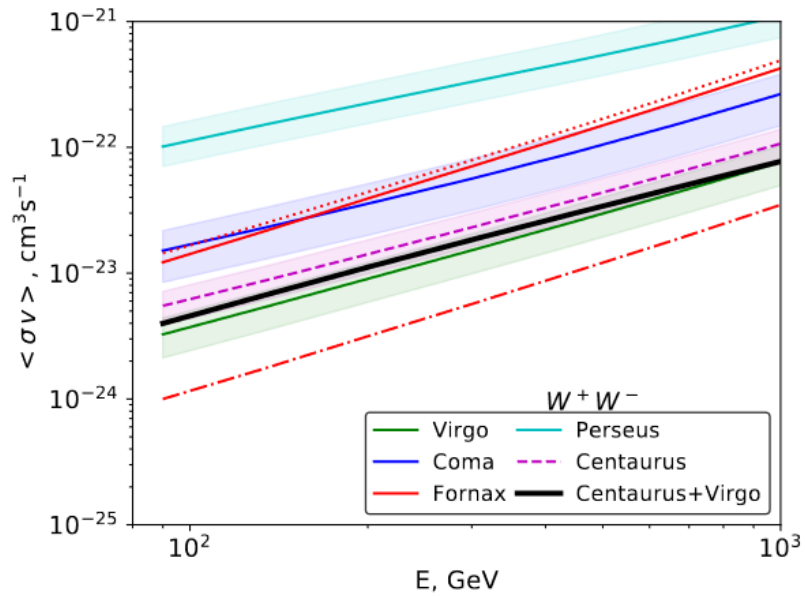
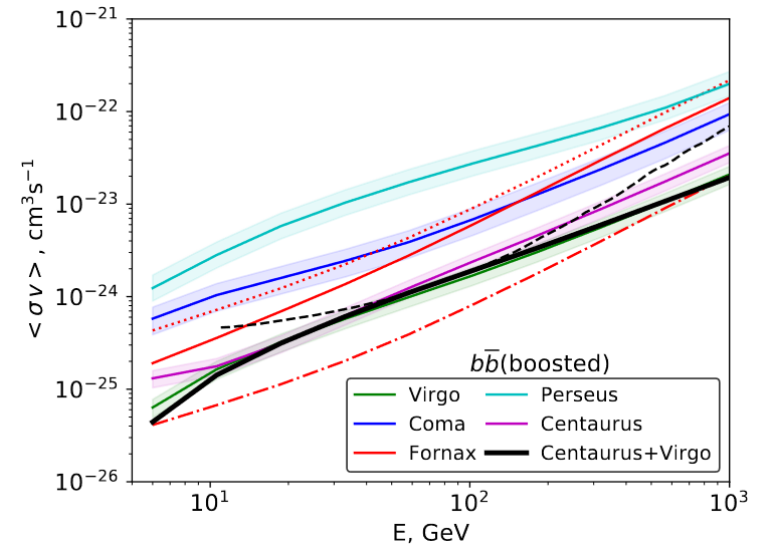


Figure 5-6: Limits on the annihilation cross-section of dark matter in the $b\bar{b}$ channel, derived from the listed galaxy clusters. Variations of the red line correspond to the differing profiles of the Fornax cluster and the dashed black line represents the limits derived by a previous study (Huang et al. 2011), included for reference. Figures left and right are limits with and without the effects of sub-structure respectively.



Results

- **No detection**
- Stacked Virgo and Centaurus observations gave the best limits
 - Formally the best found from Fornax however large discrepancy between profiles
- Strongest Cluster limits in the energy range at time of publication
 - Comparable to DSph limits (at time of publication)
 - Important crosscheck for other objects
- This work supports that clusters are viable secondary targets worth continuing to investigate





Questions?

Contact:

Charles Thorpe-Morgan

A116 - IAAT

Sand 1

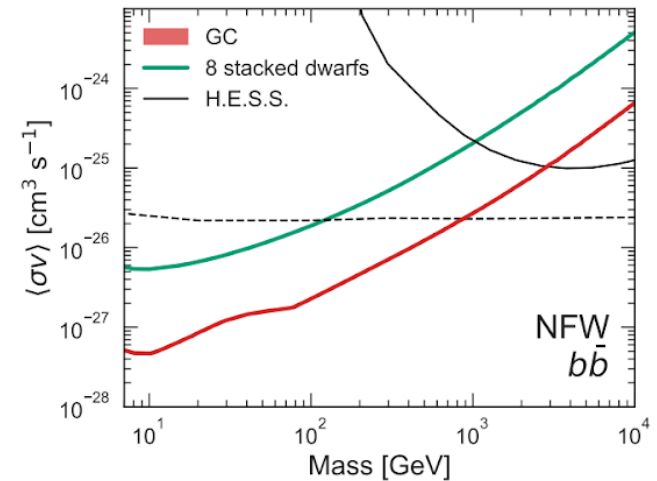
72076 Tübingen · Germany

charles.thorpe-morgan@uni-tuebingen.de

Constraints

$$\frac{d\phi(\Delta\Omega, E)}{dE} = \frac{1}{4\pi} \frac{\langle \sigma v \rangle}{2m^2} \sum B_{ri} \frac{dN_i(E)}{dE} \times \int_{\Delta\Omega} \int_{l.o.s} \rho^2 dl d\Omega$$

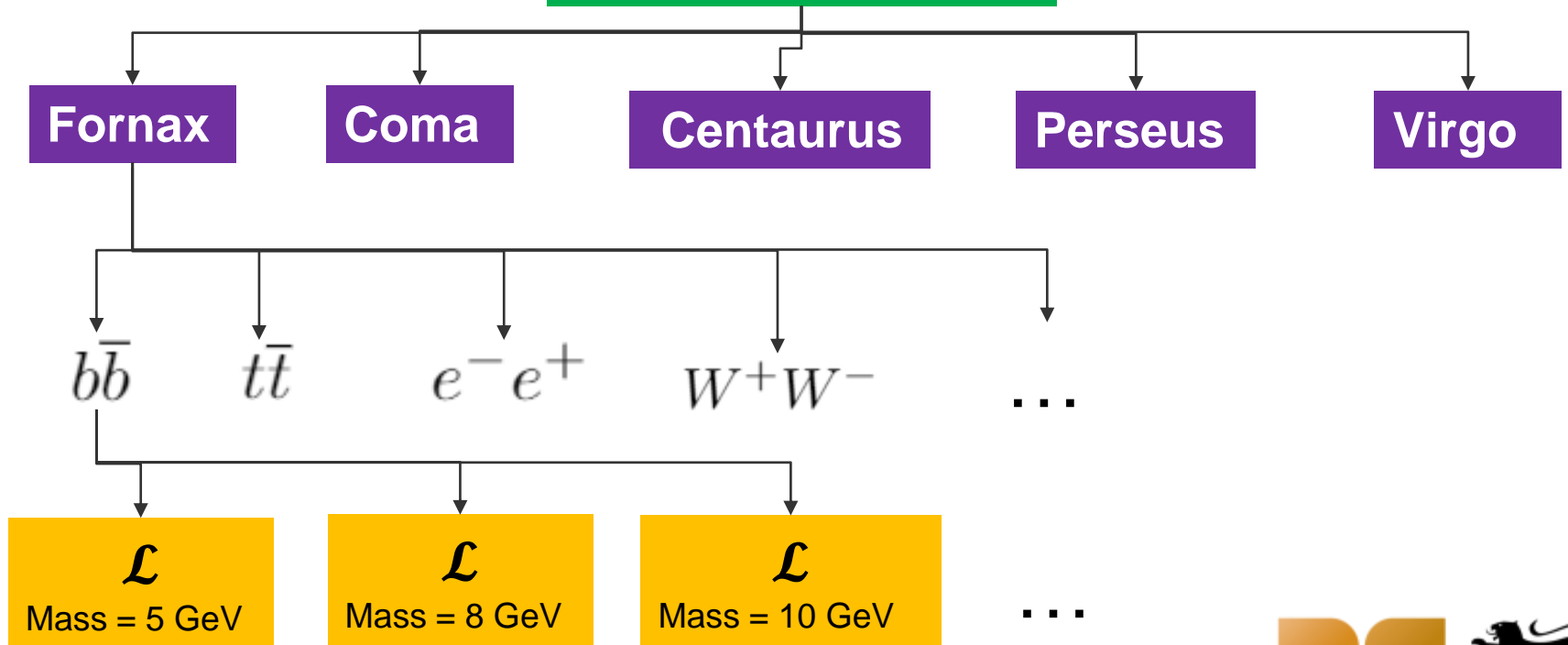
- Non-detection of DM allows constraints to be placed on the properties of DM
 - J-factor can be calculated from known quantities
 - Particle physics elements can be either simulated or assumed constant
 - By measuring the lower limits on flux seen one can derive lower limits on the annihilation cross section
- Allows comparison between different targets and to direct searches
- Allows one to build up a picture of the remaining available parameter space



Abazajian et al. 2020



Total Analysis



- For each of the 5 galaxy clusters
 - Ran a likelihood analysis in decay 10 channels
 - For each decay channel a likelihood analysis was performed for a range of DM particle mass values from 5-1000 GeV
- Required significant computational power



- Formally best constraints from Fornax
 - Profile (Reiprich Bohringer 2002) ~20 stronger limits than other Fornax profiles
 - Discounted due to this discrepancy

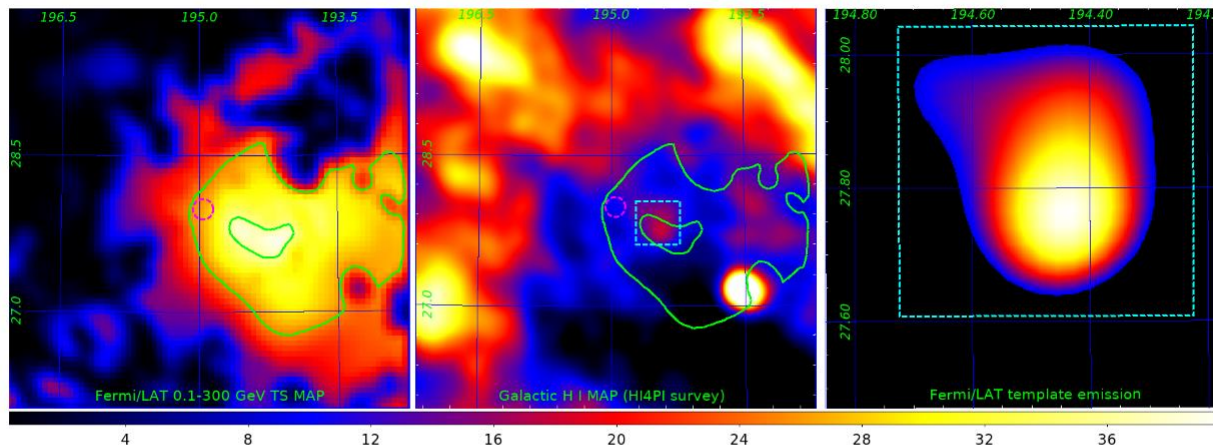


Figure 1. Left panel: Fermi/LAT test statistics map of a $2^\circ \times 2^\circ$ region around the position of the Coma cluster, shown with a dashed magenta circle. The colour scale corresponds to the square of the significance of point-like source added at each point. The bright excess seen is consistent with the results of Xi et al. (2018). Green contours represent isobars of 6σ and 7σ detection significance (moving inward respectively). Middle panel: Galactic H I map of the region from HI4PI survey HI4PI Collaboration et al. (2016). Green contours are overlaid and correspond to those of the left panel. Right panel: a template added to the model of the Coma cluster region used for Fermi/LAT data analysis. The cyan square corresponds to its counterpart in the middle panel, see text for the details.

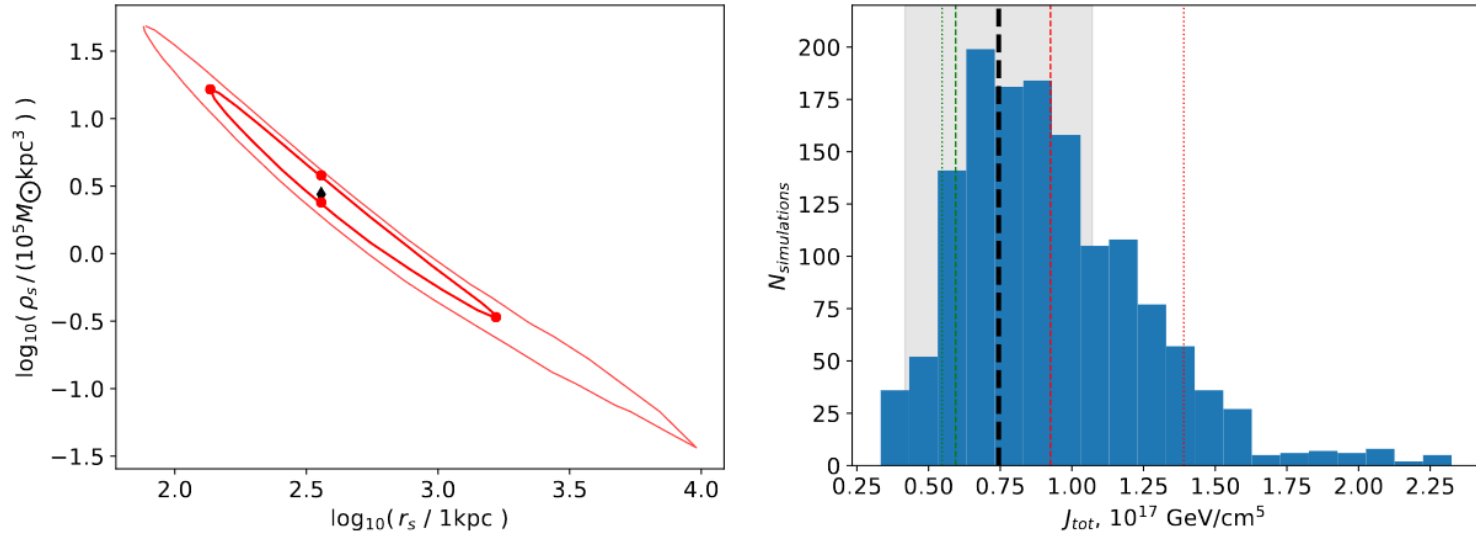


Figure 3. Left panel: The red contour represents a 1σ confidence range for r_s, ρ_s parameters of DM profile 3 of the Coma cluster, adopted from the plot within Gavazzi et al. (2009). The central black diamond corresponds to Gavazzi et al. (2009) best-fit values of r_s and ρ_s . Red square points show the characteristic parameters used for J -factor uncertainty estimations, see text for the details. Right panel: The J -factor distribution derived from 1400 points apportioned within the 1σ and 2σ contours shown in left panel. The vertical black dashed line shows the mean J -factor value corresponding to Gavazzi et al. (2009) the best-fit values of r_s and ρ_s . The grey shaded region indicates the formal dispersion of the derived distribution plotted around the mean J -factor value. Thin dotted lines correspond to red square points in the left panel, see text for the details.



Additional Sources

- NFW Profile Image, slide 8, http://people.virginia.edu/~dmw8f/astr5630/Topic05/t5_nfw.html
 - Sub-halos diagram, slide 9, <https://kids.frontiersin.org/article/10.3389/frym.2017.00029>
 - Differential Gamma-ray spectrum, slides 10,11 and 21, *Jeltema et al 2008*
 - BW HPC image, slide 24, BW HPC Website
-